*Maritime Technology and Engineering – Guedes Soares & Santos (Eds)*
*© 2015 Taylor & Francis Group, London, ISBN 978-1-138-02727-5*

# Flexural testing of sandwich laminates for steel-composite joints

L.S. Sutherland, F. Alizadeh & C. Guedes Soares
*Centre for Marine Technology and Engineering (CENTEC), Instituto Superior Técnico, Universidade de Lisboa, Lisbon, Portugal*

ABSTRACT: The material properties of four laminates with different skin/core/production method are compared in order to identify their mechanical properties. In this study, 3-point flexural beam tests following the ASTM standard C393 are carried out on each of the four laminates and the results are compared. The main experimental conclusions were that laminates with thinner skins were susceptible to core crushing and that core properties did not always correspond with published manufacturer's values. To validate a numerical procedure against experimental results an ANSYS FEA study to replicate the experimental results in terms of load-deflection curves and maximum load is carried out.

## 1 INTRODUCTION

The replacement of specific steel ship structural parts such as superstructures, transverse bulkheads, partial decks and other non-critical parts with composite materials is being studied in the EU FP7 project 'MOSAIC' (2014). The project aims to improve the structural response of the ship, and reduce corrosion, the lightship weight of the structure, and the maintenance and overall operation costs of the vessel.

The critical problem in replacing parts of a steel ship with composite structures is that of joining the two dissimilar materials together, and hence any such study will need to focus on these joints. However, before any joint design may be undertaken it is necessary to decide on exactly which composite materials will be used, both to ensure that these materials will perform well within the joint, and to ensure that the joint is designed taking into account the behaviours of the specific composite materials selected.

To ensure sufficient structural stiffness sandwich laminates were considered and discussions between the various academic and industrial partners identified four initial candidate laminates each with a specific skin/core/production method combination. Various material properties of these four candidate laminates were investigated and compared in order to help select the most promising in terms of joining composite components to the steel main structure. As part of this study 3-point flexural beam tests were carried out and these are the subject of this paper. Since core crushing was seen to be an issue in some of the tests this behaviour was investigated through Finite Element Analysis (FEA), which was validated against the experimental results.

## 2 EXPERIMENTAL RESULTS

Details of the four sandwich configurations considered (designated 'Material' 3, 4, 5 and 7) are given in Table 1.

Both upper and lower facings were of the same laminate giving a symmetrical sandwich and the reinforcement used was 813 g/m2 biaxial stitched E-glass fabric. Details of the core and composite facing resin materials are given in Table 2.

The specimens were cut to a length of 330 mm, and the other nominal and measured specimen dimensions are given in Table 3.

A calibrated servo-hydraulic mechanical test rig was used to follow ASTM C-393 (00) (ASTM 2000) "Standard Test Method for Flexural Properties of Sandwich Constructions" using a short beam three-point loading test set-up (Fig. 1).

Preliminary tests were completed using initial estimates of the required support length and roller diameter were set at 280 mm and 20 mm respectively using previous experience of similar tests and the ASTM standard as a guide. However, premature top facing failure was seen due to core crushing from excessive contact forces under the load roller, and so in order to reduce this problem a 20 mm wide steel plate was placed under the load roller and further preliminary tests made. This test set-up was successful in obtaining shear failure for the Material 5 balsa-cored specimens and hence was used for all further tests on beams of this material.

However, for the PVC-cored specimens excessive core compression was still suspected because of the low calculated core shear strengths compared to that of the manufacturer's data sheet. This was confirmed by comparing and correlating

Table 1. Sandwich ('Material') configurations.

| Material No. (Designation) | Core | Plies | Resin | Fabrication |
|---|---|---|---|---|
| 3 (HLU-G/E/PVC-F) | PVC | 2 | Epoxy | Hand layup |
| 4 (VB-G/V/PVC-F) | PVC | 4 | Vinylester | Vacuum bagging |
| 5 (VB-G/V/BAL-F) | Balsa | 4 | Vinylester | Vacuum bagging |
| 7 (VB-G/E/PVC) | PVC | 3 | Epoxy | Vacuum bagging |

Table 2. Core and facing resin materials.

| Core | Resin | Supplier | Type |
|---|---|---|---|
| PVC | – | DIAB | Divinycell H100 (100 kg/m$^3$) |
| Balsa | – | DIAB | ProBalsa Standard (155 kg/m$^3$) |
| – | Vinylester | Scott Bader | CRYSTIC VE679PA |
| – | Epoxy | West System | 105/205 Standard |

Table 3. Specimen dimensions.

| Units: (mm) | Sandwich width | Specimen thickness | Lower skin thickness |
|---|---|---|---|
| Nominal values | 70 | 35 | 2.5 |
| Average values: | | | |
| Material 3 | 70.13 | 34.10 | 2.46 |
| Material 4 | 70.07 | 35.14 | 2.35 |
| Material 5 | 70.07 | 35.07 | 2.43 |
| Material 7 | 71.25 | 35.35 | 3.01 |
| **Units: (mm)** | **Upper skin thickness** | | **Core thickness** |
| Nominal values | 2.5 | | 30 |
| Average values: | | | |
| Material 3 | 2.45 | | 29.19 |
| Material 4 | 2.56 | | 30.23 |
| Material 5 | 2.56 | | 30.08 |
| Material 7 | 2.78 | | 29.56 |

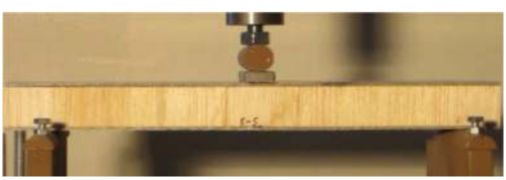

Figure 1. Experimental set-up.

force-displacement data with video recordings of the tests (Fig. 2).

Hence, for the PVC cored specimens a further round of single tests was completed using a 40 mm wide steel loading plate under the loading roller. Although, as described later, there were still concerns about core-crushing in some cases, a decision was taken to complete the remaining tests using the test set-ups given in Table 4.

This was justifiable because the only remaining way to reduce this effect was to change the laminate lay-up schedules (which were pre-specified) and since this approach would also allow consistent comparisons between the materials in terms of their flexural behaviours, which were the main thrust of this study.

ASTM C-393 (00) instructs to "Apply the load at a constant rate that will cause the maximum load to occur between 3 to 6 min". Hence, using experience obtained from the preliminary tests the test machine cross-head loading rates were set at those as also given in Table 4.

### 2.1 *Experimental results*

Five specimens of each material were tested using the set-up described in the previous section. Representative example load-deflection curves for each material are compared in Figure 3 and for individual tests for each of the four materials in Figures 4 to 7.

Balsa-cored specimens gave a sudden catastrophic 'brittle' failure and so the maximum load was used to calculate the core shear strength for these tests. However, all of the PVC-cored composite specimens were seen to yield more than 2% and hence the 2% offset method for yield strength was used as per the standard. A simple calculation assuming pure shear was used to calculate the displacement corresponding to an 'engineering' 2% shear strain of 2.80 mm. Failure modes are further detailed in the discussion. For comparative purposes shear strengths based on the maximum load were also calculated for specimens whose PVC core yielded by more than 2%. Average strength values for each material are given together with standard estimates of variability in Table 5.

Table 4. Type of loading and span.

| Material | 3 | 4 | 5 | 7 | 8 |
|---|---|---|---|---|---|
| Support length (mm) | 280 | 280 | 280 | 280 | 280 |
| Support roller Ø (mm) | 20 | 20 | 20 | 20 | 20 |
| Loading plate width (mm) | 40 | 40 | 20 | 40 | 40 |
| Cross-head rate (mm/s) | 0.05 | 0.05 | 0.015 | 0.5 | 0.5 |

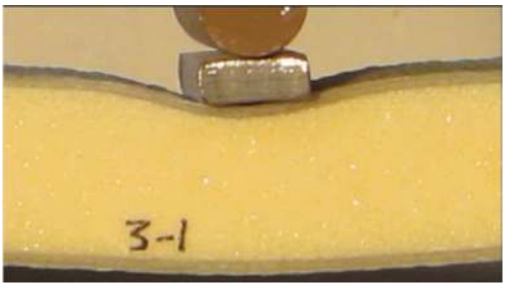


Figure 2. Local loading PVC core crushing.

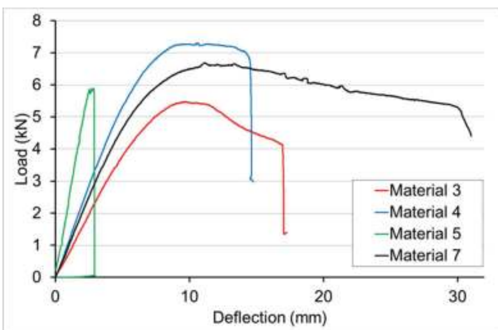


Figure 3. Example load-deflection curves.

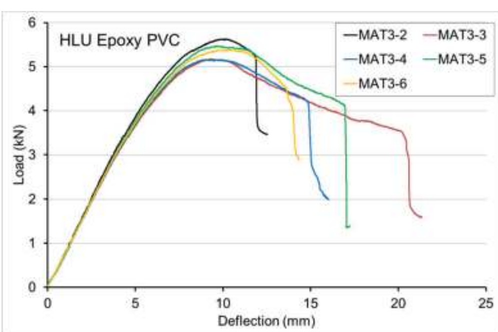


Figure 4. Material 3 load-deflection curves.

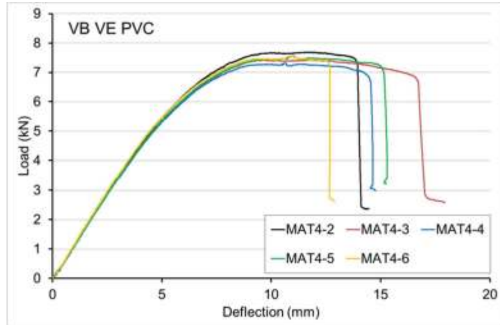


Figure 5. Material 4 load-deflection curves.

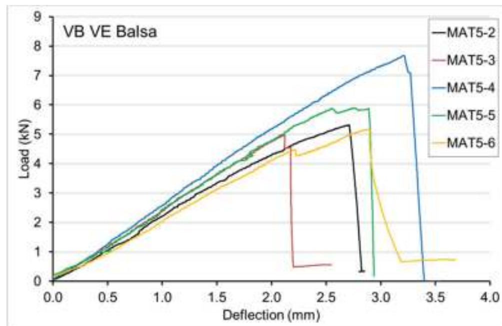


Figure 6. Material 5 load-deflection curves.

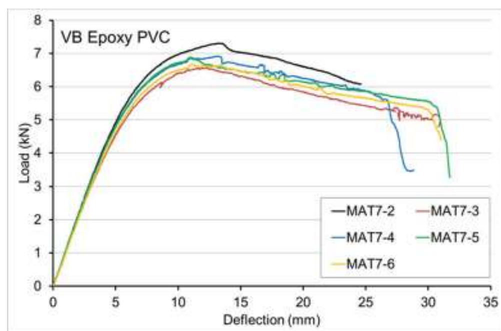


Figure 7. Material 7 load-deflection curves.

As per ASTM D-7250 (ASTM 2012), as indicated in ASTM C-393-11 (ASTM 2011), the core shear stiffness was calculated using the experimentally determined facing modulus values of Table 6 to give the panel bending stiffness, $D$ from:

$$D = \frac{E_1 t_1 E_2 t_2 (d + c)^2 b}{4(E_1 t_1 + E_2 t_2)} \tag{1}$$

Table 5. Core shear stiffness and strength results.

| | $\tau_{Fmax}$ (MPa) | $\tau_{2\% \text{ yield}}$ (MPa) | $G_{Core}$ (MPa) |
|---|---|---|---|
| *Material 3 (HLU-G/E/PVC)* | | | |
| Average | 1.21 | 1.20 | 30.8 |
| Std. Dev. | 0.04 | 0.04 | 0.6 |
| C.O.V. (%) | 3.7 | 3.7 | 2.0 |
| *Material 4 (VB-G/V/PVC)* | | | |
| Average | 1.64 | 1.62 | 43.5 |
| Std. Dev. | 0.03 | 0.03 | 0.7 |
| C.O.V. (%) | 2.0 | 1.8 | 1.6 |
| *Material 5 (VB-G/V/BAL)* | | | |
| Average | 1.27 | – | 122.1 |
| Std. Dev. | 0.23 | – | 18.0 |
| C.O.V. (%) | 18.3 | – | 14.8 |
| *Material 7 (VB-G/E/PVC)* | | | |
| Average | 1.49 | 1.41 | 35.3 |
| Std. Dev. | 0.06 | 0.05 | 1.5 |
| C.O.V. (%) | 4.0 | 3.8 | 4.2 |

Table 6. Experimental facing moduli.

| | $E_{COMP}$ (GPa) | $E_{TENS}$ (GPa) |
|---|---|---|
| Material 3 | 15.90 | 16.97 |
| Material 4 | 23.40 | 26.39 |
| Material 5 | 23.40 | 26.39 |
| Material 7 | 20.88 | 23.55 |

where: $E$ = facing modulus, $t$ = facing thickness, $d$ = sandwich thickness, $c$ = core thickness, $b$ = sandwich width, and subscripts 1 and 2 correspond to upper compressive and lower tensile values respectively.

This result for $D$ was then used together with the experimental linear load-deflection slope $P/\Delta$ and the support length $L$ to give the panel shear rigidity, $U$ from:

$$\Delta = \frac{PL^3}{48D} + \frac{PL}{4U} \quad (2)$$

The core shear modulus, $G$ was then calculated from:

$$U = \frac{G(d+c)^2 b}{4c} \quad (3)$$

The resultant average core shear modulus estimates together with standard estimates of variability are also given in Table 5.

### 2.2 *Discussion*

The failure mode of the balsa-cored composite-skinned Material 5 specimens was sudden catastrophic shear failure, both within the core itself and between the core and the facings. In only one case was it possible to identify the order of these failure modes, where frame by frame analysis of the video recording showed that failure in the core occurred shortly before core-facing de-bonding. For the other tests on this material it was impossible to ascertain the order of failure mode from the videos (shot at 24 FPS). Further, the core shear failure was seen to be either within the balsa wood itself (Fig. 8) or at a bond-line between the separate wood blocks making up the sheets of the core (Fig. 9).

The failure modes of the balsa-cored sandwich beams are given in Table 7.

The average balsa core strength of 1.3 MPa was much lower than the manufacturer's quoted value of 3.0 MPa (DIAB 2009). This could be because some specimens failed at weaker bond-lines between blocks of balsa, and that in other cases the initial failure mode was in fact de-bonding between the core and the facings. However, it is not possible to confirm this on the evidence of the current data.

The calculated core stiffness of the balsa (average 122 MPa) was also lower than the manufacturer's value of 166 MPa (DIAB 2009). Again,

Figure 8. Balsa core shear failure within wood.

Figure 9. Balsa core shear failure between 'blocks'.

Table 7. Balsa sandwich failure modes.

| Specimen | Core shear failure | Core/face De-bond | $\tau_{Ult}$ (MPa) |
|---|---|---|---|
| MAT5-2 | At block bond-line | Simultaneous | 1.16 |
| MAT5-3 | At block bond-line | Simultaneous | 1.08 |
| MAT5-4 | Within balsa wood | Simultaneous | 1.66 |
| MAT5-5 | At block bond-line | Shortly after core fail | 1.29 |
| MAT5-6 | Within balsa wood | Simultaneous | 1.14 |

Table 8. Summary of PVC sandwich failure modes.

| Material | 3 | 4 | 7 |
|---|---|---|---|
| 1st Failure mode | Core yielding/Core compression | Core yielding | Core yielding |
| 2nd Failure mode | Core yielding/Core compression | Core compression | Core compression |
| Final collapse | Compressive/Shear top facing failure | Compressive/Shear top facing failure | Compressive/Shear top facing failure |

the reason(s) behind this discrepancy is not known, but higher variation was seen between the calculated balsa core properties, which would be expected since this is a natural product.

The failure modes of the PVC-cored composite-skinned sandwich beams observed (through correlation between video recordings and analysis of load-deflection curves) are summarised in Table 8.

The PVC core strength was estimated from Material 4 results whose thicker facing laminates gave less core compression errors. This value was 1.6 MPa, equal to the value quoted by the manufacturer (DIAB 2012). The test on Material 7 gave lower core shear strength than expected indicating that core compression was still affecting the results although no visual evidence of this was seen in the video recording. However, the test on Material 3 showed that core compression under the loading plate was still significantly affecting the results. This increasing order of significance of core compression under the loading plate of Material 4 < Material 7 < Material 3 can be explained by the fact that these materials have 4, 3 and 2 plies of reinforcement in each facing respectively.

Calculating the PVC core stiffness from Material 4 results gave a value of 44 MPa, higher than that of 35 MPa quoted by the manufacturer (DIAB 2012). The reason(s) behind this higher values is (are) not known, but the assumptions made and errors in the method of calculation may be to blame. Using the Material 3 & 7 results gave values of 31 and 35 MPa respectively, closer to the manufacturer's value, but core compression errors may be significant here, especially for Material 3.

## 3 NUMERICAL ANALYSES

The experimental flexural tests on the sandwich laminates were modelled as 2-D sandwich panels using ANSYS software to give load-deflection and yield strength values which were then validated against the experimental results. Due to a lack of material data for Material 5, has not yet been included in the numerical analyses. The finite element model used is illustrated in Figure 10.

A constant mesh size along the beam length was used, and after verifying that no difference was

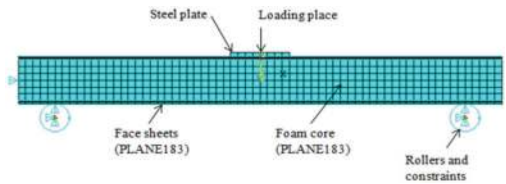


Figure 10. Finite element model.

seen in results for 1, 2 or 5 mm mesh, this was set at 5 mm. All nodes on the lower skin at 25 mm from one end of the beam were constrained in the y- and x-directions, whilst the corresponding nodes at the other end of the beam were constrained in the y- direction only. Loading was modelled using a concentrated load onto a steel loading plate, as used in the experimental tests.

The sandwich skins were modelled using the 2-D structural plane element PLANE183 with the relevant bi-linear stiffness determined from experimental data obtained as part of the MOSAIC project (Kotsidis et al. 2014) for each relevant type of skin. The sandwich core was modelled as an orthotropic material also using the 2-D structural plane element PLANE183, taking the material properties from the appropriate DIAB data sheet (DIAB 2009, 2012).

The material properties used are given in Table 9.

The obtained numerical results are compared with the experimental force-displacement curves in Figure 11.

Figure 11(b) shows that for PVC-cored Material 4 the FEA predicts the experimental behaviour seen very well, using the material properties obtained from material characterisation testing, without the need for any 'calibration'. This is also the case for the balsa-cored sandwich laminate Material 5 as shown in Figure 11(c).

However, the numerical prediction of the PVC-cored Material 3 experimental behaviour is seen in Figure 11(a) to be much too stiff. This is apparently because the FEA does not correctly predict the 'plastic' like behaviour due core compression under the load application plate seen in the experiments. It is thought that further refinement of the core compression material properties is required

Table 9. Material properties of FE model (E, G and σ in MPa).

| Material | $E_1$ | $E_2$ | $E_3$ | $\upsilon_{12}$ | $\upsilon_{13}$ |
|---|---|---|---|---|---|
| HLU-G/E | 16972 | 3000 | 15994 | 0.5 | 0.25 |
| VB-G/V | 26393 | 3000 | 25217 | 0.5 | 0.25 |
| VB-G/E | 23545 | 3000 | – | 0.5 | 0.25 |
| Divinycell H100 | 131 | 59.8 | 59.8 | 0.4 | 0.4 |
| Pro Balsa standard | 4100 | 125.5 | 125.5 | 0.36 | 0.36 |

| Material | $\upsilon_{23}$ | $G_{12}$ | $G_{13}$ | $G_{23}$ | $E_{tan}$ | $\sigma_{yield}$ |
|---|---|---|---|---|---|---|
| HLU-G/E | 0.05 | 1000 | 2140 | 1000 | 400 | 324.5 |
| VB-G/V | 0.05 | 1204 | 2204 | 1204 | 527 | 445.1 |
| VB-G/E | 0.05 | 823 | 1823 | 823 | 471 | 357.2 |
| Divinycell H100 | 0.4 | 32.5 | 32.5 | 20 | 1.62 | 2.55 |
| Pro Balsa standard | 0.23 | 166 | 166 | 20.5 | 82 | 13.1 |

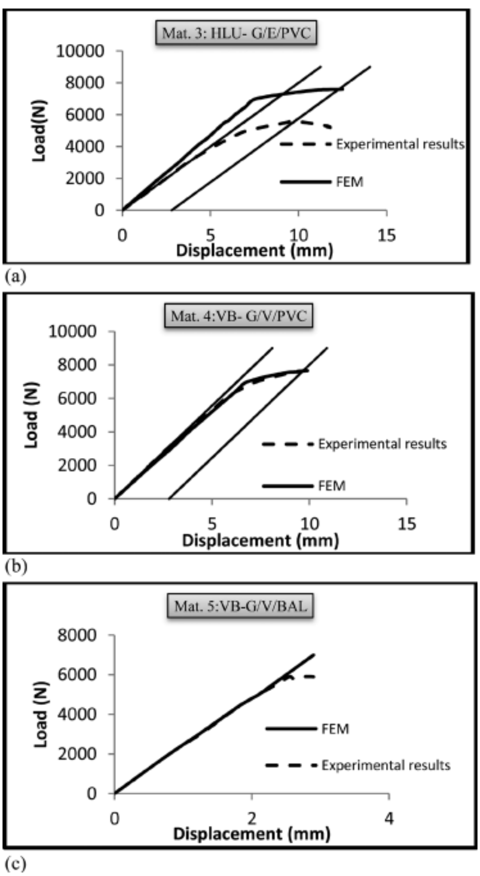


Figure 11. FEA vs. experimental load-deflection behaviour.

Table 10. 2% shear strain offset yield strengths.

| | Mat. 3 | | Mat. 4 | |
|---|---|---|---|---|
| Material | FEM | Test | FEM | Test |
| Strength (kN) | 7.7 | 5.6 | 7.6 | 7.6 |
| % Error | 62 | | 7 | |

to rectify this. However, since tests (or in-service behaviour) where this core compression occurs are not considered valid (or desirable) then this is perhaps not worth pursuing.

Table 10 compares the numerically and experimentally obtained values of ultimate strength calculated at the 2% shear strain offset yield stress, where it can again be seen that results are only accurate for Material 4 whose stiffer skins helped resist local core compression.

## 4 CONCLUSIONS

Material property data concerning the shear core stiffnesses and strengths has been obtained.

The PVC core material properties were best estimated from Material 4 results whose thicker facing laminates resisted local loading core compression. The measured PVC core shear strength value was 1.6 MPa, equal to the value quoted by the manufacturer (DIAB 2012). The calculated Material 4 PVC core stiffness was 44 MPa, higher than that of 35 MPa quoted by the manufacturer (DIAB 2012). The reason(s) behind this higher value is (are) not known, but the assumptions made in the method of calculation may be to blame. Using the Material 7 results gave the manufacturer's value of 35 MPa, but core compression errors were thought to be significant here.

The average balsa core strength of 1.3 MPa was much lower than the manufacturer's quoted value of 3.0 MPa (DIAB 2009). This could be because some specimens failed at weaker bond-lines between blocks of balsa, and that in other cases the initial failure mode was in fact debonding between the core and the facings. However, it is not possible to confirm this on the evidence of the current data.

The calculated core stiffness of the balsa (average 122 MPa) was also lower than the manufacturer's value of 166 MPa (DIAB 2012). Again, the reason(s) behind this discrepancy is not known, but higher variation was seen between the calculated balsa core properties, which could be expected from a natural product.

Comparisons of the various flexural behaviours seen, including the influence of skin thickness/stiffness on susceptibility to contact loads for

PVC-cored materials and differences in shear failure modes between PVC and Balsa cored composite skinned sandwich beam, together with the material properties obtained, enabled the project to select a most suitable candidate sandwich material to take forward into the next component-scale steel to composite laminate joint analysis and testing phase.

The numerical analyses completed using ANSYS gave promising initial results for the load deflection behaviour and core yield strength of sandwich laminates where local loading core compression was not significant. This was achieved using the actual material properties obtained from material characterisation testing, without the need for any 'calibration'. In order to further investigate local loading core crushing numerically, more complete core properties and compression behaviour would be required.

## ACKNOWLEDGEMENTS

This work has been done within the project 'Materials Onboard: Steel Advancement and Integrated Composites—MOSAIC', (www.mosaicships.com), which was partially funded by the European Community's Seventh Framework Programme under grant No. 314037.

## REFERENCES

ASTM Standard C 393-00, "Standard Test Method for Flexural Properties of Sandwich Constructions", ASTM International, West Conshohocken, PA, 2000.

ASTM Standard C393/C393M-11e1, "Standard Test Method for Core Shear Properties of Sandwich Constructions by Beam Flexure", ASTM International, West Conshohocken, PA, 2011.

ASTM D7250/D7250M-06(2012), "Standard Practice for Determining Sandwich Beam Flexural and Shear Stiffness", ASTM International, West Conshohocken, PA, 2012.

DIAB Data Sheet, "Divinycell H Technical Data", H-ds.10_2012.rev8, DIAB Group, Laholm, Sweden, 2012.

DIAB Data Sheet, "ProBalsa Technical Data", ProBalsa-ds.09_2009.rev, DIAB Group, Laholm, Sweden, 2009.

Kotsidis, E.A., Kouloukouras, I.G. and Tsouvalis, N.G., MOSAIC Report "*Composite materials manufacturing and characterization*" 2014.

"Materials Onboard: Steel Advancement and Integrated Composites—MOSAIC" (www.mosaicships.com) 2014.